PAPER www.rsc.org/dalton | Dalton Transactions

Correlating Pt–P bond lengths and Pt–P coupling constants†

Paul G. Waddell, Alexandra M. Z. Slawin and J. Derek Woollins*

Received 16th February 2010, Accepted 8th June 2010
DOI: 10.1039/c003256e

The X-ray structures of (**5**) *cis*-PtBr$_2$(P(OMe)$_3$)$_2$, (**6**) *cis*-PtBr$_2$(P(OMe)$_2$Ph)$_2$, (**7**) *cis*-PtBr$_2$(P(OMe)Ph$_2$)$_2$, (**8**) *cis*-PtBr$_2$(PPh$_3$)$_2$, (**9**) *cis*-PtI$_2$(P(OMe)$_3$)$_2$, (**10**) *cis*-PtI$_2$(P(OMe)$_2$Ph)$_2$, (**11**) *cis*-PtI$_2$(P(OMe)Ph$_2$)$_2$ and (**12**) *cis*-PtI$_2$(PPh$_3$)$_2$ are reported and compared with the previously reported chloride analogues. The magnitude of the J\{Pt–P\} varies linearly with the Pt–P bond length ($l_{\text{Pt–P}} = 2.421 - J/24255$) for these 12 complexes.

Introduction

As a consequence of their interesting reactivity and since the discovery of the anticancer action of *cis*-platin[1] the study of square planar platinum complexes has been of great interest. Platinum complexes containing phosphorus ligands are of particular interest as their ^{31}P NMR spectra contain ^{195}Pt satellite peaks which allow the ^{31}P–^{195}Pt coupling constant to be measured giving insight into the nature of bonding around the platinum centre.[2] Previous studies have shown in a limited range of compounds that there is a crude correlation between the P–Pt bond length and the ^{31}P–^{195}Pt coupling constant.[3–5] Here we report the crystal structures of a series of *cis*-PtX$_2$(P(OMe)$_n$Ph$_{3-n}$)$_2$ (X = Br or I; n = 0–3) and compare them to their *cis*-PtCl$_2$(P(OMe)$_n$Ph$_{3-n}$)$_2$ analogues to create a series with coupling constants in the range 3450–5750 Hz and show that the relationship between their ^{31}P–^{195}Pt coupling constant and Pt–P bond length is linear.

Experimental

Unless otherwise stated all manipulations were performed under an oxygen-free nitrogen atmosphere, using standard Schlenk techniques and glassware. Solvents were dried and stored according to common procedures. Reagents were obtained from Aldrich and used without further purification. Solution state ^{31}P–\{^{1}H\} (109 MHz, Table 1) and ^{1}H (270 MHz) NMR spectra were recorded using a JEOL GSX Delta 270. IR spectra were recorded using KBr discs on a Perkin-Elmer System 2000 FT spectrometer. Microanalyses were performed by the University of St. Andrews microanalysis service.

cis-PtBr$_2$(P(OMe)$_3$)$_2$,[6] *cis*-PtBr$_2$(P(OMe)$_2$Ph)$_2$,[7] *cis*-PtBr$_2$(P(OMe)Ph$_2$)$_2$[7] and *cis*-PtBr$_2$(PPh$_3$)$_2$[8] were prepared in good yield from *trans*-PtBr$_2$(PhCN)$_2$ and two equivalents of the phosphite, phosphonite, phosphinite or phosphine in acetone. *cis*-PtI$_2$(P(OMe)$_3$)$_2$[6] was prepared in good yield from *trans*-PtI$_2$(PhCN)$_2$ and two equivalents of trimethyl phosphite in acetone. *cis*-PI$_2$(PPh$_3$)$_2$[8] was prepared by metathesis of *cis*-PtCl$_2$(PPh$_3$)$_2$ with excess sodium iodide in an equivolume mixture of water, ethanol, acetone and chloroform. All compounds were characterised using NMR. Crystals suitable for X-ray crystallography were grown by slow diffusion of hexane into a solution of the complex in dichloromethane for all except *cis*-PtBr$_2$(PPh$_3$)$_2$ (grown by slow diffusion of hexane into a solution of the complex in chloroform).

Preparation of *cis*-PtI$_2$(P(OMe)$_2$Ph)$_2$

1 g (1.53 mmol) of *trans*-PtI$_2$(PhCN)$_2$ was vigorously stirred in 40 mL acetone to which 0.48 mL (3.05 mmol) of P(OMe)$_2$Ph was added affording a clear yellow solution. The volume of acetone was reduced to *ca.* 10 mL with a yellow precipitate of *cis*-PtI$_2$(P(OMe)$_2$Ph)$_2$ forming. The remaining product was precipitated upon addition of 50 mL diethyl ether. The solid was filtered and washed with diethyl ether to give a crystalline, yellow solid, mp 172–174°. Crystals were grown for X-ray crystallography by slow diffusion of hexane into a solution of the product in dichloromethane. Yield: 0.632 g (0.8 mmol), 52%. Elemental Analysis (%, calculated in brackets): C, 24.65 (24.35); H, 2.51 (2.81). ^{1}H NMR (CDCl$_3$, 291 K): $\delta_{\text{(ppm)}} = 3.66$ (d, 12H, methyl, $^3J_{\text{PH}} = 12.9$ Hz), $\delta_{\text{(ppm)}} = 7.41$–7.77 (m, 10H, phenyl). ^{31}P\{^{1}H\} NMR (C$_6$D$_6$, 295 K): $\delta_{\text{(ppm)}} = 96.4$ ($^1J_{\text{ P–Pt}} = 4618$ Hz). Infra red: $\nu_{\text{Pt–I}}$ 163, 150 cm^{-1}, $\nu_{\text{Pt–P}}$ 202, 188 cm^{-1}, $\nu_{\text{P–O-alkyl}}$ 1045 cm^{-1}, $\nu_{\text{P–Ph}}$ 1434 cm^{-1}.

Preparation of *cis*-PtI$_2$(P(OMe)Ph$_2$)$_2$

1 g (1.53 mmol) of *trans*-PtI$_2$(PhCN)$_2$ was vigorously stirred in 40 mL acetone to which 0.61 mL (3.05 mmol) of P(OMe)Ph$_2$ was added affording a clear yellow solution. The volume of acetone was reduced to *ca.* 10 mL with a yellow precipitate of *cis*-PtI$_2$(P(OMe)$_2$Ph)$_2$ forming. The solid was filtered and washed with diethyl ether to give a yellow powder, mp 182–186°. Crystals were grown for X-ray crystallography by slow diffusion of hexane into a solution of the product in dichloromethane. Yield: 1.255 g (1.43 mmol), 93%. Elemental Analysis (%, calculated in brackets): C, 35.52 (35.42); H, 2.66 (2.97).^{1}H NMR (CDCl$_3$, 291 K): $\delta_{\text{(ppm)}} =$ 3.31 (d, 6H, methyl, $^3J_{\text{PH}} = 12.4$ Hz), $\delta_{\text{(ppm)}} = 7.36$–7.79 (m, 20H, phenyl). ^{31}P\{^{1}H\} NMR (C$_6$D$_6$, 295 K): $\delta_{\text{(ppm)}} = 83.5$ ($^1J_{\text{ P–Pt}} = 3995$ Hz). Infra red: $\nu_{\text{Pt–I}}$ 175, 167 cm^{-1}, $\nu_{\text{Pt–P}}$ 218, 206 cm^{-1}, $\nu_{\text{P–O–alkyl}}$ 1032 cm^{-1}, $\nu_{\text{P–Ph}}$ 1436 cm^{-1}.

Crystallography

Crystal structure data (Tables 2–4) were collected for all complexes at 125 K using a Rigaku SCX-Mini, (Mo radiation). All data was

---

School of Chemistry, University of St Andrews, St Andrews, Scotland KY16 9ST. E-mail: jdw3@st-and.ac.uk

† CCDC reference numbers 766308–766315. For crystallographic data in CIF or other electronic format see DOI: 10.1039/c003256e

Table 1 ^{31}P NMR chemical shifts and ^{195}Pt–^{31}P coupling constants for (**1**)–(**12**)

Compound	δ_{ppm}	J_{P-Pt}/Hz
(**1**) *cis*-$PtCl_2(P(OMe)_3)_2$	73.7	5707
(**2**) *cis*-$PtCl_2(P(OMe)_2Ph)_2$	97.2	4819
(**3**) *cis*-$PtCl_2(P(OMe)Ph_2)_2$	85.2	4183
(**4**) *cis*-$PtCl_2(PPh_3)_2$	14.5	3679
(**5**) *cis*-$PtBr_2(P(OMe)_3)_2$	75.2	5662
(**6**) *cis*-$PtBr_2(P(OMe)_2Ph)_2$	97.0	4777
(**7**) *cis*-$PtBr_2(P(OMe)Ph_2)_2$	84.9	4141
(**8**) *cis*-$PtBr_2(PPh_3)_2$	14.0	3627
(**9**) *cis*-$PtI_2(P(OMe)_3)_2$	77.6	5477
(**10**) *cis*-$PtI_2(P(OMe)_2Ph)_2$	96.4	4618
(**11**) *cis*-$PtI_2(P(OMe)Ph_2)_2$	83.5	3995
(**12**) *cis*-$PtI_2(PPh_3)_2$	11.6	3472

corrected for absorption. The structures were solved by direct methods and refined by full-matrix least-squares methods on F^2 values of all data.[9] Refinements were performed using SHELXL.[10]

Results and discussion

The crystal structures and ^{31}P NMR for the dichloride complexes have been previously reported [(**1**) *cis*-$PtCl_2(P(OMe)_3)_2$,[5] (**2**) *cis*-$PtCl_2(P(OMe)_2Ph)_2$,[11] (**3**) *cis*-$PtCl_2(P(OMe)Ph_2)_2$[12] and (**4**) *cis*-$PtCl_2(PPh_3)_2$].[13] The dibromide and diiodide analogues [(**5**) *cis*-$PtBr_2(P(OMe)_3)_2$, (**6**) *cis*-$PtBr_2(P(OMe)_2Ph)_2$, (**7**) *cis*-$PtBr_2(P(OMe)Ph_2)_2$, (**8**) *cis*-$PtBr_2(PPh_3)_2$, (**9**) *cis*-$PtI_2(P(OMe)_3)_2$, (**10**) *cis*-$PtI_2(P(OMe)_2Ph)_2$, (**11**) *cis*-$PtI_2(P(OMe)Ph_2)_2$ and (**12**) *cis*-$PtI_2(PPh_3)_2$] were characterised in this work.

The ^{31}P–$\{^1H\}$ NMR spectra of all the complexes (Table 1) exhibit singlets together with satellites due to $^1J_{Pt-P}$ couplings. For each of the three halides the coupling constant is observed to decrease in the order $P(OMe)_3 > P(OMe)_2Ph > P(OMe)Ph_2 > PPh_3$ (Fig. 1) as the π-acidity of the phosphorus ligands decrease. In addition to this, for each of the four phosphorus ligands the coupling constant decreases in the order Cl > Br > I as the degree of π back-bonding between the platinum and the halide, and hence the halide's ability to compete with the phosphorus for the electron back-donation, increases. This can be interpreted as an increase in *trans*-influence as the coupling constant is an indication of bond strength and *trans*-influence is defined as the ability of a ligand to weaken the bond *trans* to it.[14] The chemical shifts are also seen to decrease in the order Cl > Br > I with the exception of the complexes containing $P(OMe)_3$ where the opposite is observed.

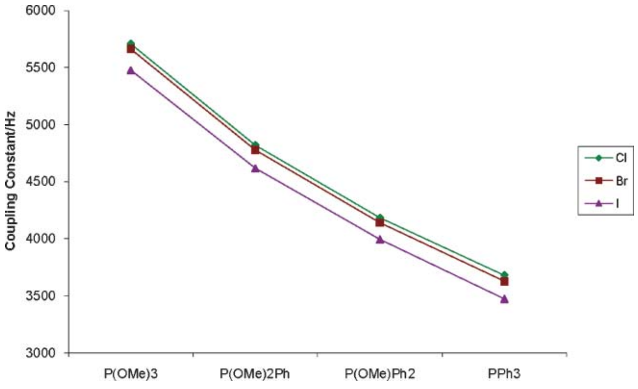

Fig. 1 Variation of ^{195}Pt–^{31}P coupling constants with phosphite/phosphine character.

The X-ray crystal structures of the dibromide complexes (**5**)–(**8**) (Fig. 2, Table 2) were determined and refined to a good standard. All of the structures exhibit square planar geometry about the platinum and were observed to be isostructural to their dichloride analogues. The Pt–Br distances lie within the range 2.4696(4) Å to 2.4933(5) Å and exhibit no significant trend. The Pt–P bond lengths are within the range 2.207(2) Å to 2.2685(10) Å and, as was observed in the dichloride analogues, increase in the order $P(OMe)_3 < P(OMe)_2Ph < P(OMe)Ph_2 < PPh_3$. The P(1)–Pt–P(2) and Br(1)–Pt–Br(2) bond angles lie in the ranges 93.74(9)° to 98.41(4)° and 86.000(18)° to 89.265(17)° respectively with no significant trends apparent.

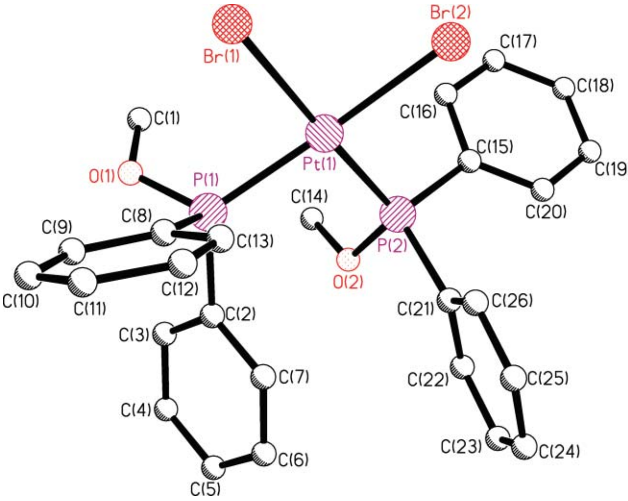

Fig. 2 X-ray crystal structure of (**7**). The structures of (**5**), (**6**) and (**8**) are not illustrated as they are similar.

The X-ray crystal structures of the diiodide complexes (**9**)–(**12**) (Fig. 3, Table 2) were also determined and observed to be isostructural though not necessarily isomorphous to the dibromide structures. Similar trends in bond lengths and angles as those observed for the dibromides are also evident. Most significantly

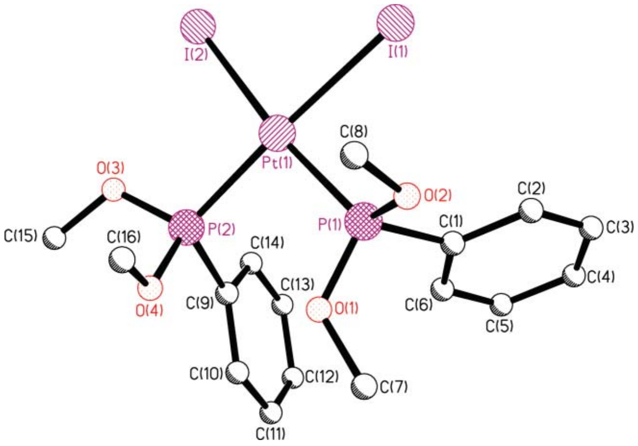

Fig. 3 X-ray crystal structure of (**10**). The structures of (**9**), (**11**) and (**12**), are not illustrated as they are similar.

Table 2 Selected bond lengths (Å) and angles (°) for (**1**)–(**12**)

	(**1**) $PtCl_2(P(OMe)_3)_2$[5]	(**2**) $PtCl_2(P(OMe)_2Ph)_2$[11]	(**3**) $PtCl_2(P(OMe)Ph_2)_2$[12]	(**4**) $PtCl_2(PPh_3)_2$[13]
Pt–Cl(1)	2.384(4)	2.3625(9)	2.3693(12)	2.3632(8)
Pt–Cl(2)	2.408(4)	2.3625(9)	2.3533(12)	2.3294(9)
Pt–P(1)	2.192(3)	2.2193(9)	2.2272(11)	2.2713(9)
Pt–P(2)	2.155(3)	2.2193(9)	2.2279(12)	2.2515(8)
P(1)–Pt–P(2)	95.5(1)	101.16(3)	98.14(4)	99.12(3)
Cl(1)–Pt–Cl(2)	85.8(1)	89.08(3)	89.37(4)	87.56(3)

	(**5**) $PtBr_2(P(OMe)_3)_2$	(**6**) $PtBr_2(P(OMe)_2Ph)_2$	(**7**) $PtBr_2(P(OMe)Ph_2)_2$	(**8**) $PtBr_2(PPh_3)_2$
Pt–Br(1)	2.4742(11)	2.4933(5)	2.4895(4)	2.4696(4)
Pt–Br(2)	2.4753(11)	2.4762(4)	2.4828(5)	2.4859(5)
Pt–P(1)	2.217(2)	2.2161(9)	2.2400(11)	2.2625(13)
Pt–P(2)	2.207(2)	2.2248(12)	2.2424(11)	2.2685(10)
P(1)–Pt–P(2)	93.74(9)	93.76(4)	98.41(4)	97.55(4)
Br(1)–Pt–Br(2)	88.54(3)	89.209(16)	89.265(17)	86.000(18)

	(**9**) $PtI_2(P(OMe)_3)_2$	(**10**) $PtI_2(P(OMe)_2Ph)_2$	(**11**) $PtI_2(P(OMe)Ph_2)_2$	(**12**) $PtI_2(PPh_3)_2$
Pt–I(1)	2.6587(4)	2.6608(5)	2.6814(5)	2.6647(6)
Pt–I(2)	2.6571(4)	2.6569(4)	2.6533(5)	2.6448(5)
Pt–P(1)	2.2214(14)	2.2360(14)	2.2481(19)	2.295(2)
Pt–P(2)	2.2248(16)	2.244(2)	2.2518(19)	2.277(2)
P(1)–Pt–P(2)	94.56(5)	93.84(6)	93.01(7)	97.47(7)
I(1)–Pt–I(2)	88.979(13)	88.836(17)	88.003(17)	87.456(18)

Table 3 Experimental and refinement details for the X-ray structures for (**5**)–(**8**)

Compound	(**5**)	(**6**)	(**7**)	(**8**)·$CHCl_3$
Fw	$C_6H_{18}O_6P_2Br_2Pt$	$C_{16}H_{22}O_4P_2Br_2Pt$	$C_{26}H_{26}O_2P_2Br_2Pt$	$C_{37}H_{31}P_2Cl_3Br_2Pt$
M	603.05	695.19	787.34	998.86
T/K	125	125	125	125
Crystal System	Orthorhombic	Triclinic	Monoclinic	Triclinic
Space group	$Pna2_1$	$P\bar{1}$	$P\,2_1/n$	$P\bar{1}$
a/Å	12.6116(9)	9.1545(7)	12.675(3)	11.1265(7)
b/Å	7.6773(6)	9.9510(8)	13.753(5)	11.7130(7)
c/Å	16.0931(12)	13.1489(10)	14.938(10)	14.2633(10)
α (°)	90	110.452(8)	90	90.826(6)
β (°)	90	94.763(7)	93.283(9)	98.341(7)
γ (°)	90	108.745(8)	90	106.986(8)
U/Å^3	1558.2(2)	1036.72(14)	2599.6(20)	1755.81(20)
Z	4	2	4	2
μ(Mo-Kα)mm^{-1}	14.328	10.778	8.604	6.608
D_c/Mg m^{-3}	2.570	2.227	2.012	1.889
Total reflections	12415	3629	22176	15229
Independent	2730	3641	4568	6155
Reflections (R_{int})	(0.085)	(0.026)	(0.050)	(0.036)
Max and min. transmission	0.4333, 0.2386	0.3575, 0.1904	0.2776, 0.2071	0.5297, 0.2587
Final R,R′	0.0335, 0.0664	0.0203, 0.0449	0.0265, 0.0624	0.0353, 0.0842
Largest difference	1.36	0.49	1.16	1.00
peak, hole/e.Å^{-3}	–0.92	–0.69	–0.99	–0.88

the Pt–P bond lengths (2.2214(14) Å to 2.295(2) Å) increase in the order $P(OMe)_3 < P(OMe)_2Ph < P(OMe)Ph_2 < PPh_3$. The Pt–I distances are in the range 2.6448(5) Å to 2.6814(5) Å and the P(1)–Pt–(P2) and Br(1)–Pt–Br(2) bond angles lie in the ranges 88.979(13)° to 97.47(7)° and 87.456(18)° to 94.56(5)° respectively with the latter decreasing in the order $P(OMe)_3 > P(OMe)_2Ph > P(OMe)Ph_2 > PPh_3$.

Comparing the structures of compounds (**1**)–(**12**) it can be seen that for each of the halides the Pt–P bond length is seen to increase in the order $P(OMe)_3 < P(OMe)_2Ph < P(OMe)Ph_2 < PPh_3$ with the PPh_3 complexes having Pt–P bond lengths *ca.* 0.06 Å longer than the $P(OMe)_3$ complexes (Table 2, Fig. 4). For each of the phosphorus ligands the Pt–P bond length increases in the order Cl < Br < I with Pt–P bond lengths in the iodide complexes being *ca.* 0.03 Å longer than their dichloride equivalents. These two effects are in accord with [1] the π-acidity of the phosphorus ligands increasing as the oxygen content rises and [2] the heavier halogens being better π-acceptors and thus phosphorus *trans* to iodine is less strongly bound than phosphorus *trans* to chloride.

When considering the magnitude of the {Pt–P} coupling constant the s-character of the orbitals involved in the Pt–P bond is usually considered to be the most important variable.

Table 4 Experimental and refinement details for the X-ray structures for (**9**)–(**12**)

Compound	(**9**)	(**10**)	(**11**)	(**12**)·H_2O
Fw	$C_6H_{18}O_6P_2I_2Pt$	$C_{16}H_{22}O_4P_2I_2Pt$	$C_{26}H_{26}O_2P_2I_2Pt$	$C_{36}H_{32}OP_2I_2Pt$
M	697.05	789.19	881.34	991.49
T/K	125	125	125	125
Crystal System	Monoclinic	Triclinic	Monoclinic	Triclinic
Space group	$P2_1/n$	$P\bar{1}$	Cc	$P\bar{1}$
a/Å	9.0554(4)	9.496(3)	10.456(4)	9.8227(5)
b/Å	14.7571(7)	10.044(3)	17.143(7)	10.4994(6)
c/Å	12.8733(9)	13.743(4)	15.597(6)	17.7427(13)
α (°)	90	66.910(15)	90	86.757(6)
β (°)	98.251(7)	71.546(18)	104.500(3)	77.704(6)
γ (°)	90	71.621(15)	90	70.376(5)
U/Å^3	1702.46(16)	1116.0(6)	2706.7(19)	1683.78(17)
Z	4	2	4	2
μ(Mo-Kα)mm^{-1}	12.035	9.189	7.585	6.107
D_c/Mg m^{-3}	2.719	2.348	2.163	1.955
Total reflections	14469	9745	11522	14529
Independent	2993	3922	4748	5893
Reflections (R_{int})	(0.051)	(0.035)	(0.035)	(0.046)
Max and min. transmission	0.5837, 0.2200	0.2602, 0.2062	0.7023, 0.4157	0.6088, 0.4408
Final R,R′	0.0276, 0.0472	0.0287, 0.0625	0.0267, 0.0467	0.0403, 0.0922
Largest difference peak, hole/e.Å^{-3}	0.76 −0.93	1.25 −1.66	0.94 −1.00	2.02 −1.15

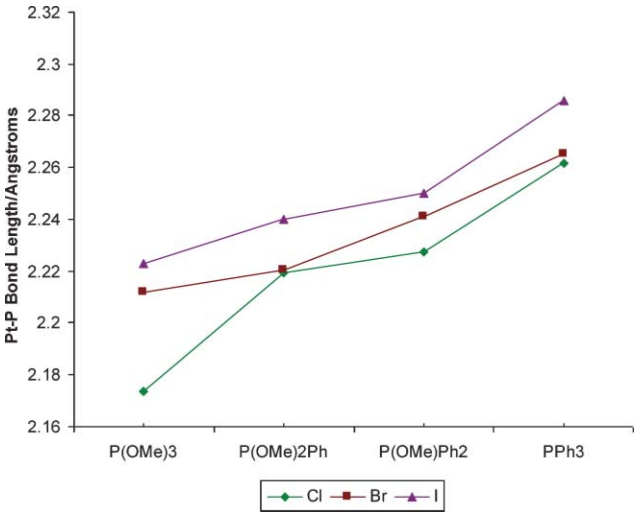

Fig. 4 Variation of Pt–P in $PtX_2(P(OMe)_nPh_{3-n})_2$ complexes.

$$^1J_{(M-P)} = \gamma_M\gamma_P\frac{64\pi^2}{9}\beta^2\frac{|S_M(0)|^2}{\Delta E}|S_P(0)|^2(P'_{S_MS_P})^2 \qquad (1)$$

Thus, to a good approximation, the coupling constant is given by eqn (1)[3] where the s-characters of the orbitals is contained in the M.O. bond order between the s-orbitals, $(P'_{S_MS_P})^2$. The valance state s-orbital basis functions are given by the expressions $|S_P(0)|$ and $|S_M(0)|$, ΔE is the average excitation energy and γ_M and γ_P the magnetogyric constants for each nucleus. As is evident the principles involved are complex however for a given phosphorus ligand and metal centre $|S_P(0)|$ and $|S_M(0)|$ should remain relatively constant leaving $(P'_{S_MS_P})^2$ as the dominating factor in the magnitude of $^1J_{Pt-P}$. Clearly given eqn (1), provided the nature of the bonding is not dramatically different there should be a good correlation between Pt–P bond length and $J\{$Pt–P$\}$.

We found that as the bond length increases the coupling constant decreases. The correlation between these two measurements in this series of compounds is rather good giving a reasonable straight line that can be fitted by eqn (2) (Fig. 5). We did consider that another way of gauging the s-character and hence the strength of the bond would be to look at the R–P–R, R–P–O and O–P–O bond angles in these complexes with larger values indicating a move towards more ideal sp^3 hybridisation however we did not observe any correlation in this regard.. It thus appears that in a narrow series of complexes the coupling constant could be used as a good indicator of bond length.

$$l_{(Pt-P)} = 2.421 - \frac{J}{24255} \qquad (2)$$

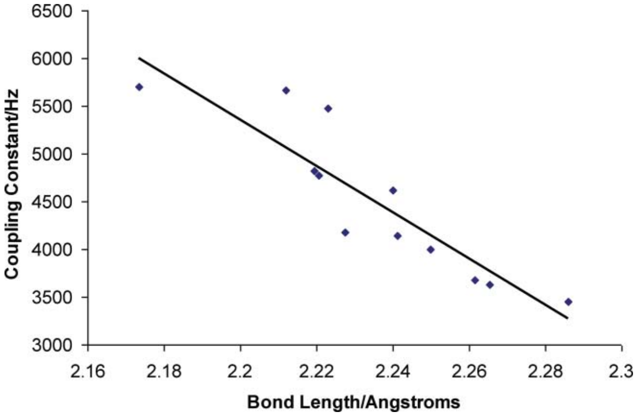

Fig. 5 Correlation of $^1J_{Pt-P}$ with Pt–P bond length in $PtX_2(P(OMe)_nPh_{3-n})_2$ complexes.

To further test the principle we compared Pt–P bond lengths and $^1J_{Pt-P}$ coupling constants we examined $Pt(E_2N_2)(PR_3)_2$[15–21] as well as their protonated equivalents that have been prepared in our and other labs,[18,20–25] corresponding *cis*- and *trans*-dihalides[26–48]

Table 5 Pt–P distances and Coupling constants used in Fig. 6

Compound (*trans*-atom in bold)	Pt–P Bond Length/Å	$^1J_{Pt\text{–}P}$/Hz
$Pt(S_2\mathbf{N}_2)(P(OPh)_3)_2$[15]	2.221(3)	4634
$Pt(\mathbf{S}_2N_2)(P(OPh)_3)_2$	2.234(3)	4503
$Pt(S_2\mathbf{N}_2)(P(OMe)_3)_2$[15]	2.217(3)	4502
$Pt(\mathbf{S}_2N_2)(P(OMe)_3)_2$	2.246(3)	4395
$Pt(S_2\mathbf{N}_2)(P(OEt)_3)_2$[15]	2.239(2)	4498
$Pt(\mathbf{S}_2N_2)(P(OEt)_3)_2$	2.237(2)	4415
$Pt(S_2\mathbf{N}_2)(P(OMe)_2Ph)_2$[15]	2.2175(15)	3864
$Pt(\mathbf{S}_2N_2)(P(OMe)_2Ph)_2$	2.2407(15)	3761
$Pt(S_2\mathbf{N}_2)(P(OMe)Ph_2)_2$[15]	2.250(2)	3287
$Pt(\mathbf{S}_2N_2)(P(OMe)Ph_2)_2$	2.256(2)	3249
$Pt(S_2\mathbf{N}_2)(PPh_3)_2$	2.263(4)[16]	2994[17]
$Pt(\mathbf{S}_2N_2)(PPh_3)_2$	2.317(4)	2827
$Pt(S_2\mathbf{N}_2)(PMe_2Ph)_2$	2.265(3)[18]	2799[17]
$Pt(\mathbf{S}_2N_2)(PMe_2Ph)_2$	2.271(4)	2731
$Pt(S_2\mathbf{N}_2)(PMePh_2)_2$	2.243(2)[19]	2886[17]
$Pt(\mathbf{S}_2N_2)(PMePh_2)_2$	2.281(2)	2781
$Pt(S_2\mathbf{N}_2)(PMe_3)_2$	2.261(6)[17]	2748[17]
$Pt(\mathbf{S}_2N_2)(PMe_3)_2$	2.268(5)	2681
$[Pt(S_2\mathbf{N}_2H)(PMe_2Ph)_2]PF_6$	2.262(2)[18]	3240[22]
$[Pt(\mathbf{S}_2N_2H)(PMe_2Ph)_2]PF_6$	2.305(2)	2595
$[Pt(S_2\mathbf{N}_2H)(PMe_3)_2]PF_6$	2.249(1)[23]	3130[22]
$[Pt(\mathbf{S}_2N_2H)(PMe_3)_2]PF_6$	2.263(1)	2566
$[Pt(S_2\mathbf{N}_2H)(PEt_3)_2]PF_6$	2.270(3)[24]	3162[22]
$[Pt(\mathbf{S}_2N_2H)(PEt_3)_2]PF_6$	2.320(3)	2563
$[Pt(S_2\mathbf{N}_2H)(P^nBu_3)_2]_2[PF_6]Cl$[22]	2.2675(2)	3164
$[Pt(\mathbf{S}_2N_2H)(P^nBu_3)_2]_2[PF_6]Cl$	2.3145(2)	2561
$Pt(SeS\mathbf{N}_2)(P(OMe)_3)_2$[15]	2.243(2)	4530
$Pt(\mathbf{Se}SN_2)(P(OMe)_3)_2$	2.214(2)	4571
$Pt(SeS\mathbf{N}_2)(P(OMe)_2Ph)_2$[15]	2.2480(14)	3868
$Pt(\mathbf{Se}SN_2)(P(OMe)_2Ph)_2$	2.2266(13)	3900
$Pt(SeS\mathbf{N}_2)(P(OMe)Ph_2)_2$[15]	2.260(3)	3309
$Pt(\mathbf{Se}SN_2)(P(OMe)Ph_2)_2$	2.253(4)	3391
$Pt(SeS\mathbf{N}_2)(PPh_3)_2$[15]	2.3069(17)	2996
$Pt(\mathbf{Se}SN_2)(PPh_3)_2$	2.2664(12)	2948
$Pt(SeS\mathbf{N}_2)(PMe_2Ph)_2$	2.271(2)[20]	2799[21]
$Pt(\mathbf{Se}SN_2)(PMe_2Ph)_2$	2.261(2)	2837
$[Pt(SeS\mathbf{N}_2H)(PMe_2Ph)_2]BF_4$	2.262(2)[20]	2687[21]
$[Pt(\mathbf{Se}SN_2H)(PMe_2Ph)_2]\ BF_4$	2.301(2)	3227
$[Pt(TeS\mathbf{N}_2H)(PMe_2Ph)_2]\ BF_4$[25]	2.257(3)	2645
$[Pt(\mathbf{Te}SN_2H)(PMe_2Ph)_2]\ BF_4$	2.313(3)	3171
cis-$PtCl_2(P(OEt)_3)_2$	2.2235	5697
cis-$PtCl_2(P(O^iPr)_3)_2$[26]	2.21465	5812
cis-$PtCl_2(P(OPh)_3)_2$	2.19915[27]	5793
cis-$PtCl_2(P(OMe)_3)_2$	2.1735[5]	5707
cis-$PtCl_2(P(OMe)_2Ph)_2$[11]	2.2190	4819
cis-$PtCl_2(P(OMe)Ph_2)_2$[12]	2.22755	4183
cis-$PtCl_2(PPh_3)_2$	2.2614[13]	3679
cis-$PtCl_2(PMe_3)_2$	2.238[28]	3489[29]
cis-$PtCl_2(PMe_2Ph)_2$	2.244[30]	3549[31]
cis-$PtCl_2(PMePh_2)_2$	2.24875[32]	3616[31]
cis-$PtCl_2(PEt_3)_2$	2.263[33]	3520[31]
cis-$PtCl_2(PEt_2Ph)_2$	2.25295[34]	3530[31]
cis-$PtCl_2(PEtPh_2)_2$	2.25745[35]	3640[31]
cis-$PtCl_2(dppe)_2$[36]	2.208	3610
cis-$PtCl_2(dppp)_2$[36]	2.232	3408
cis-$PtBr_2(P(OPh)_3)_2$	2.205[37]	5728[38]
cis-$PtI_2(PMe_3)_2$	2.2575[39]	3317[29]
cis-$PtI_2(dppe)_2$	2.2418[40]	3366[41]
trans-$PtCl_2(PEt_3)_2$	2.298[42]	2400[31]
trans-$PtCl_2(P^iPr_3)_2$	2.3392[43]	2417[44]
trans-$PtCl_2(PPh_3)_2$	2.3186[45]	2630[46]
trans-$PtI_2(PPh_3)_2$	2.318[47]	2496[46]
trans-$PtI_2(PMe_3)_2$	2.315[48]	2236[29]
cis-$Pt(NSO)_2(PPh_3)_2$	2.3278[49]	3027[50]
cis-$Pt(NSO)_2(PMe_3)_2$[50]	2.263	3190

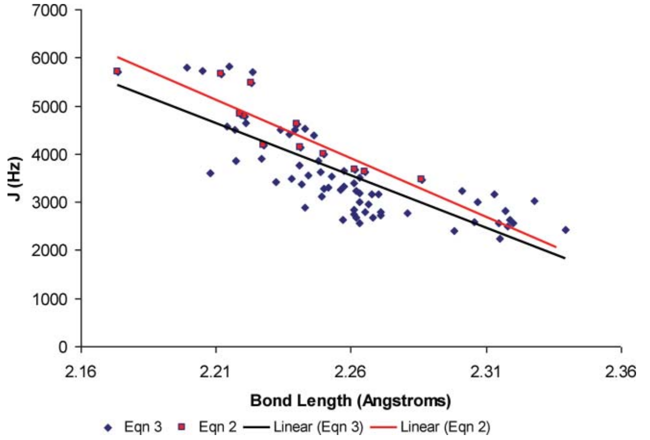

Fig. 6 Correlation of $^1J_{Pt\text{–}P}$ with Pt–P bond length in large range of Pt–Phosphorus complexes. Black line is best fit to the points in the graph eqn (3). Red line is the line from eqn (2).

Table 6 Coupling constants and calculated (using eqn (2) or (3)) and observed bond lengths for selected compounds

Compound	$^1J_{Pt\text{–}P}$/Hz	$l_{Pt\text{–}P}$/Å	Eqn 2 (Å)	Eqn 3 (Å)
$[Pt(9S3)(PPh_3)Cl]PF_6$[51]	3387	2.2838(8)	2.281	2.266
$[Pt(10S3)(PPh_3)Cl]PF_6$[51]	3438	2.285(2)	2.279	2.264
$[Pt(PMe_3)_2\{CS_3\}]$[52]	2969	2.265	2.298	2.285
$[Pt(PPh_3)_2\{CS_3\}]$[52]	3145	2.2915	2.29	2.278
$[Pt(dppp)_2\{CS_3\}]$[52]	2881	2.263	2.302	2.289
$[Pt(Se_2naph)(P(OPh)_3)_2]$[53]	4711	2.231	2.227	2.208

and $Pt(NSO)_2(PR_3)_2$ complexes.[49,50] This supports the assertion (Fig. 6, Table 5) that the larger the coupling constant the shorter the Pt–P bond length. As can be seen in Fig. 6 the correlation is not necessarily linear since at the extremes significant energetic stabilisation is needed in order to influence bond length and the magnitude of coupling constants is a better measure of s orbital overlap than of absolute bond length, however the best fit straight line is given by eqn (3).

$$l_{(Pt-P)} = 2.422 - \frac{J}{21827} \qquad (3)$$

Using eqn (2) and (3) we tested the accuracy of the correlation as an indicator of bond length on a selection of compounds (Table 6). It is interesting to note that in most cases eqn (2) tends to give a more accurate result than eqn (3) the former being on average within 0.015 Å of the observed distance and the latter within 0.02 Å. The accuracy of eqn (3) could potentially be improved with a more extensive literature search.

References

1 B. Rosenberg, L. Van Camp and T. Krigas, *Nature*, 1965, **205**(4972), 698.
2 A. Pidcock, *Advances in Chemistry Series*, 1982, **196**, (Catal. Aspects Met. Phosphine Complexes), 1.
3 G. G. Mather, A. Pidcock and G. J. N. Rapsey, *J. Chem. Soc., Dalton Trans.*, 1973, 2095.
4 R. J. Blau and J. H. Espenson, *Inorg. Chem.*, 1986, **25**, 878.
5 Q.-B. Bao, S. J. Geib, A. L. Rheingold and T. B. Brill, *Inorg. Chem.*, 1987, **26**, 3453.
6 M. J. Church and M. J. Mays, *J. Inorg. Nucl. Chem.*, 1971, **33**, 253.
7 D. Couch, S. D. Robinson and J. N. Wingfield, *J. Chem. Soc., Dalton Trans.*, 1974, 1309.
8 S. H. Mastin, *Inorg. Chem.*, 1974, **13**(4), 1003.

9 Rigaku (2006). *Crystal Structure*, Version 3.8. Single Crystal Structure Analysis Software. Rigaku/MSC, 9009 TX, USA 77381-5209. Rigaku, Tokyo 196-8666, Japan.

10 G. M. Sheldrick, *Acta Cryst*, 2008, **A64**, 112.

11 A. M. Z. Slawin, P. G. Waddell and J. D. Woollins, *Acta. Cryst.*, 2007, **E63**(7), m2017.

12 A. M. Z. Slawin, P. G. Waddell and J. D. Woollins, *Acta. Cryst.*, 2007, **E63**(7), m2018.

13 H.-K. Fun, S. Chantrapromma, Y.-C. Liu, Z.-F. Chen and H. Liang, *Acta. Cryst.*, 2006, **E62**(6), m1252.

14 T. G. Appleton, H. C. Clark and L. E. Manzer, *Coord. Chem. Rev.*, 1973, **10**, 335.

15 P. G. Waddell, A. M. Z. Slawin and J. D. Woollins, *Eur. J. Chem. Soc.*, 2010, **20**, 3185.

16 R. Jones, P. F. Kelly, D. J. Williams and J. D. Woollins, *Polyhedron*, 1985, **4**(11), 1947.

17 P. A. Bates, M. B. Hursthouse, P. F. Kelly and J. D. Woollins, *J. Chem. Soc., Dalton Trans.*, 1986, 2367.

18 R. Jones, P. F. Kelly, D. J. Williams and J. D. Woollins, *J. Chem. Soc., Dalton Trans.*, 1988, 803.

19 B. D. Read, A. M. Z. Slawin and J. D. Woollins, *Acta Cryst*, 2007, **E63**, m751.

20 C. A. O'Mahoney, I. P. Parkin, D. J. Williams and D. J. Woollins, *Polyhedron*, 1989, **8**, 2215.

21 I. P. Parkin and J. D. Woollins, *J. Chem. Soc., Dalton Trans.*, 1990, 925.

22 R. Jones, C. P. Warrens, D. J. Williams and J. D. Woollins, *J. Chem. Soc., Dalton Trans.*, 1987, 907.

23 R. Jones, P. F. Kelly, C. P. Warrens, D. J. Williams and J. D. Woollins, *J. Chem. Soc., Chem. Commun.*, 1986, 711.

24 R. Jones, C. P. Warrens, D. J. Williams and J. D. Woollins, *Acta Cryst*, 1988, **C 44**, 1381.

25 P. F. Kelly, A. M. Z. Slawin, D. J. Williams and J. D. Woollins, *Polyhedron*, 1990, **9**, 2659.

26 A. M. Z. Slawin, P. G. Waddell and J. D. Woollins, *Acta Cryst.*, 2009, **E65**, m1392.

27 S. J. Sabounchei and A. Naghipour, *Molecules*, 2001, **6**, 777.

28 A. Del Pra and G. Zanotti, *Cryst. Struct. Commun.*, 1979, **8**, 737.

29 R. R. Favez Roulet, A. A. Pinkerton and D. Schwarzenbach, *Inorg. Chem.*, 1980, **19**, 1356.

30 W. M. Attia, G. Balducci and M. Calligaris, *Acta Cryst*, 1987, **43**, 1053.

31 S. O. Grim, R. L. Keiter and W. McFarlane, *Inorg. Chem.*, 1967, **6**, 1133.

32 K. C. Ho, G. M. McLaughlin, M. McPartlin and G. B. Robertson, *Acta. Cryst.*, 1982, **B38**, 421.

33 S. Otto and A. J. Muller, *Acta. Cryst.*, 2001, **C57**, 1405.

34 W. Domanska-Babul, J. Pikies and J. Chojnacki, *Acta Cryst*, 2007, **E63**, m2583.

35 W. Domanska-Babul, J. Chojnacki and J. Pikies, *Acta Cryst.*, 2007, **E63**, m1956.

36 R. Mas-Ballesté, G. Aullón, P. Champkin, W. Clegg, C. Mégret, P. González-Duarte P. and A. Lledós, *Chem.–Eur. J.*, 2003, **9**, 5023.

37 S. J. Sabounchei and A. Naghipour, *Proc – Indian Acad. Sci. Sect. A.*, 2001, **13**, 1011.

38 N. Ahmad, E. W. Ainscough, T. A. James and S. D. Robinson, *J. Chem. Soc., Dalton Trans.*, 1973, 1148.

39 P. B. Hitchcock, B. Jacobson and A. Pidcock, *J. Organomet. Chem.*, 1977, **133**, 273.

40 N. P. Rath, V. S. S. Kumar, M. Janka and G. K. Anderson, *Inorg. Chim. Acta*, 2007, **360**, 2997.

41 I. M. Al-Najjar, *Inorg. Chim. Acta*, 1987, **128**, 93.

42 G. G. Messmer and E. L. Amma, *Inorg. Chem.*, 1966, **5**, 1775.

43 G. B. Robertson, P. A. Tucker and W. A. Wickramasinghe, *Aust. J. Chem.*, 1986, **39**, 1495.

44 J. A. Rahn, L. Baltusis and J. H. Nelson, *Inorg. Chem.*, 1990, **29**, 750.

45 M. H. Johansson and S. Otto, *Acta Cryst.*, 2000, **C56**, e12.

46 L. Rigamonti, C. Manassero, M. Rusconi, M. Manassero and A. Pasini, *Dalton Trans.*, 2009, 1206.

47 N. M. Boag, K. M. Rao and N. J. Terrill, *Acta Cryst.*, 1991, **C47**, 1064.

48 P. B. Hitchcock, B. Jacobson and A. Pidcock, *J. Chem. Soc., Dalton Trans.*, 1977, 2038.

49 R. Short, M. B. Hursthouse, T. G. Purcell, J. D. Woollins, I., 1987, 407.

50 I. P. Parkin, A. M. Z. Slawin, D. J. Williams and J. D. Woollins, *Polyhedron*, 1989, **8**(6), 835.

51 G. J. Grant, D. F. Galas and D. G. VanDerveer, *Polyhedron*, 2002, **21**, 879.

52 S. M. Aucott, A. M. Z. Slawin and J. D. Woollins, *Polyhedron*, 2000, **19**, 499.

53 A. L. Fuller, F. R. Knight, A. M. Z. Slawin and J. D. Woollins, *Eur. J. Inorg. Chem.*, submitted.